Proceedings of the 2003 IEEE International Frequency Control Symposium and PDA Exhibition Jointly with the 17th European Frequency and Time Forum

^{87}Rb and ^{133}Cs LASER COOLED CLOCKS : TESTING THE STABILITY OF FUNDAMENTAL CONSTANTS

F. Pereira Dos Santos, H. Marion, M. Abgrall, S. Zhang, Y. Sortais, S. Bize, I. Maksimovic, D. Calonico,*
J. Grünert, C. Mandache,† C. Vian, P. Rosenbuch, P. Lemonde, G. Santarelli, Ph. Laurent, and A. Clairon
BNM-SYRTE, Observatoire de Paris, 61 Avenue de l'Observatoire, 75014 Paris, France

C. Salomon
Laboratoire Kastler Brossel, ENS, 24 rue Lhomond, 75005 Paris, France

Abstract - **Over five years we have compared the hyperfine frequencies of ^{133}Cs and ^{87}Rb atoms in their electronic ground state using several laser cooled ^{133}Cs and ^{87}Rb atomic fountains with an accuracy of $\sim 10^{-15}$. These measurements set a stringent upper bound to a possible fractional time variation of the ratio between the two frequencies : $\frac{d}{dt}\ln\left(\frac{\nu_{\mathbf{Rb}}}{\nu_{\mathbf{Cs}}}\right) = (0.2 \pm 7.0) \times 10^{-16}\,\mathbf{yr}^{-1}$ (1σ uncertainty). The same limit applies to a possible variation of the quantity $(\mu_{\mathbf{Rb}}/\mu_{\mathbf{Cs}})\alpha^{-0.44}$, which involves the ratio of nuclear magnetic moments and the fine structure constant. To improve this test, one needs more accurate cesium fountain clocks, for which the major limiting factor is the cold collision frequency shift. This effect can now be evaluated with great accuracy using a new method which we also present here. It is based on a transfer of population by adiabatic passage that allows to prepare cold atomic samples with a well defined ratio of atomic density and atom number. This method is used to perform a measurement of the cold collision frequency shift in a laser cooled cesium clock at the percent level. With improvements, the adiabatic passage would allow measurements of density-dependent phase shifts at the 10^{-3} level in high precision experiments. With this precision, reaching an accuracy of 10^{-16} is possible.**

Keywords - **frequency comparison, cesium, rubidium, atomic fountain clock, adiabatic passage, fundamental constants**

Since Dirac's 1937 formulation of his large number hypothesis aiming at tying together the fundamental constants of physics [1], large amount of work has been devoted to test wether these constants were indeed constant over time [2, 3].

In General Relativity and in all metric theories of gravitation, variations with time and space of non gravitational fundamental constants are forbidden. They would violate Einstein's Equivalence Principle (EEP), one of the cornerstones of modern physics. Among several important principles, EEP imposes the Local Position Invariance stating that in a local freely falling reference frame, the result of any local non gravitational experiment is independent of where and when it is performed. On the other hand, almost all modern theories aiming at unifying gravitation with the three other fundamental interactions, introducing extra-dimensions and extra fields, predict violation of EEP at levels which are within reach of near-future experiments [4, 5]. Among these constants, the fine structure constant α is of particular interest as it is dimensionless. It is defined as $\alpha = e^2/4\pi\epsilon_0\hbar c$ where e is the electron charge, ϵ_0 the dielectric permeability of the vacuum, $\hbar$ the Planck's constant divided by 2π, and c the speed of light in vacuum. α characterizes the strength of the electromagnetic interaction, as it quantifies how the electron binds to atoms and molecules. As the internal energies of atoms or molecules depend on electromagnetic, as well as strong and weak interactions, comparing the frequency of electronic transitions, fine structure transitions and hyperfine transitions as a function of time or gravitational potential provides an interesting test of the validity of EEP.

To date, very stringent tests exist on geological and cosmological timescales. First, the study of the isotopic and geochemical composition of soil samples taken from an uranium mine in Oklo (Gabon) revealed that a natural nuclear reaction occurred there about 2×10^9 years ago. Samples from Oklo revealed a relative abundance of Samarium-149 unusually low with respect to its natural abundance everywhere on earth. This was attributed to the radiative capture of neu-

trons by Samarium-149 : ${}^{149}_{62}Sm + n \rightarrow {}^{150}_{62} Sm + \gamma$, a reaction whose scattering cross-section exhibits a resonance. This resonance energy depends on α, so does the depletion of Samarium-149, whose value was used to evaluate the variation of α between now and the time of that reaction. The analysis revealed that any fractional change in the value of α cannot be greater than 10^{-7} [6]. Today, it is the most stringent test of the stability of the fine structure constant. Astrophysical tests allow to go back even further in the past. The light emitted by distant quasars can be used to perform absorption spectroscopy of interstellar clouds at different red-shifts. For instance, measurements of the wavelengths of molecular hydrogen transitions test a possible variation of the electron to proton mass ratio m_e/m_p [7]. Comparisons between the gross structure and the fine structure of neutral atoms and ions would indicate that α for a redshift $z \sim 1.5$ (~ 10 Gyr) differed from the present value: $\Delta\alpha/\alpha = (-7.2 \pm 1.8) \times 10^{-6}$ [8]. Today this is the only claim that fundamental constants might change.

On much shorter timescales, several tests using frequency standards have already been performed, comparing for example H-masers and superconducting-cavity stabilized oscillator clocks [9], Mg and Cs atomic beam standards [10], a H-maser and a mercury ion clock [11]. These laboratory tests have a very high sensitivity to changes in fundamental constants. Moreover, they have the advantage over the previously mentioned geochemical and astrophysical tests that they are repeatable, and that systematic errors can be tracked as one can change the experimental conditions.

In the first part of this article, we present results that place a new stringent limit to the time variation of fundamental constants. By comparing the hyperfine energies of ^{133}Cs and ^{87}Rb in their electronic ground state over a period of nearly five years, we place an upper limit to the rate of change of the ratio of the hyperfine frequencies $\nu_{\rm Rb}/\nu_{\rm Cs}$. Our measurements take advantage of the high accuracy ($\sim 10^{-15}$) of several laser cooled Cs and Rb atomic fountains. According to recent atomic structure calculations [11, 12], these measurements are sensitive to a possible variation of the quantity $(\mu_{\rm Rb}/\mu_{\rm Cs})\alpha^{-0.44}$, where μ's are the nuclear magnetic moments.

In our experiments, three atomic fountains are compared to each other, using a hydrogen maser (H-maser) as a flywheel oscillator (Fig.1). Two fountains, a transportable fountain FOM, and FO1 [13] are using cesium atoms and reach an accuracy of 8×10^{-16}. The third fountain is a dual fountain (DF) [14] , operating alternately with rubidium ($\rm DF_{Rb}$) and cesium ($\rm DF_{Cs}$). This fountain has been continuously upgraded, its accuracy has improved from 2×10^{-15} in 1998 to 8×10^{-16} for cesium and from 1.3×10^{-14} [15] to 7×10^{-16} for rubidium.

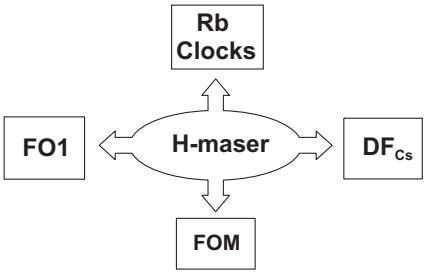

FIG. 1: BNM-SYRTE clock ensemble. A single 100 MHz signal from a H-maser is used for frequency comparisons and is distributed to each of the microwave synthesizers of the ^{133}Cs (FO1, FOM, $\rm DF_{Cs}$) and ^{87}Rb fountain clocks. In 2001, the Rb fountain has been upgraded and is now a dual fountain using alternately rubidium ($\rm DF_{Rb}$) or cesium atoms ($\rm DF_{Cs}$).

We now briefly describe the principle of operation of a laser cooled fountain clock (see Figure 2). We start by collecting up to 10^9 cold atoms in an optical molasses during a few hundred ms. The atoms are then launched upwards at about 4 m/s, further cooled to about 1 μK and then selected in the clock level ($m_F = 0$) by a combination of microwave and laser pulses. After the selection, the atoms interact twice with a microwave field tuned near the hyperfine frequency, in a Ramsey interrogation scheme. The microwave field at 9.192 GHz is synthesized from a high stability quartz oscillator weakly locked to the output of a H-maser (Fig.1). The two $\pi/2$ Ramsey interactions are separated by 500 ms. After the microwave interactions, the number of atoms in each hyperfine state are finally measured by detecting the fluorescence induced by a pair of laser beams located below the molasses region. This provides a measurement of the transition probability as a function of microwave detuning. Successive measurements are used to steer the average microwave field to the frequency of the atomic resonance using a digital servo system. The output of the servo provides a direct measurement of the frequency difference between the H-maser and the fountain clock.

The three fountains have different geometries and

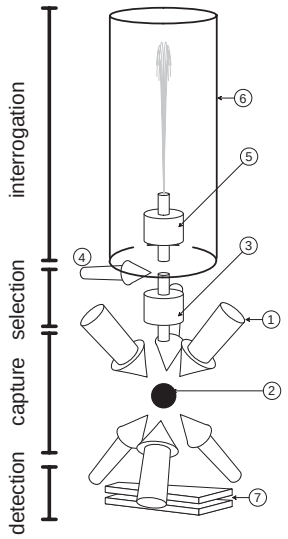

FIG. 2: Scheme of a fountain clock. 1 : one of the six laser beams, 2 : optical molasses, 3 : selection microwave cavity, 4 : pusher laser beam, 5 : interrogation cavity, 6 : magnetic shield, 7 : fluorescence detection laser beams

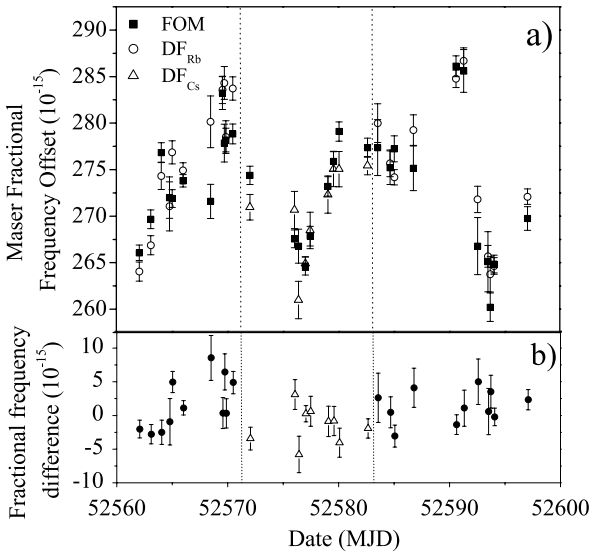

FIG. 3: The 2002 frequency comparison data. a) H-maser fractional frequency offset versus FOM (■), and alternately versus DF_{Rb} (○) and DF_{Cs} (△ between dotted lines). b) Fractional frequency differences. Between dotted lines, Cs-Cs comparisons, outside Rb-Cs comparisons. Error bars are purely statistical. They correspond to the Allan standard deviation of the comparisons and do not include contributions from fluctuations of systematic shifts of Table I.

operating conditions : the number of detected atoms ranges from 3×10^5 to 2×10^6 at a temperature of $\sim 1\,\mu$K, the fountain cycle duration from 1.1 to 1.6 s. The Ramsey resonance width is between 0.9 and 1.2 Hz. In measurements reported here the fractional frequency instability is $(1-2) \times 10^{-13}\tau^{-1/2}$, where τ is the averaging time in seconds. Fountain comparisons have a typical resolution of $\sim 10^{-15}$ for a 12 hour integration, and each of the four data campaigns lasts from 1 to 2 months during which an accuracy evaluation of each fountain is performed.

The 2002 measurements are presented in Fig.3, which displays the maser fractional frequency offset, measured by the Cs fountains FOM and DF_{Cs}. Also shown is the H-maser frequency offset measured by the Rb fountain DF_{Rb} where the Rb hyperfine frequency is conventionally chosen to be $\nu_{Rb}(1999) = 6\,834\,682\,610.904\,333$ Hz, our 1999 value. The data are corrected for the systematic frequency shifts listed in Table I. The H-maser frequency exhibits fractional frequency fluctuations on the order of 10^{-14} over a few days, ten times larger than the typical statistical uncertainty resulting from the instability of the fountain clocks. In order to reject the H-maser frequency fluctuations, the fountain data are recorded simultaneously (within a few minutes). The fractional frequency differences plotted in Fig.3 b illustrate the efficiency of this rejection. DF is operated alternately with Rb and Cs, allowing both Rb-Cs comparisons and Cs-Cs comparisons (central part of Fig.3) to be performed.

Systematic effects shifting the frequency of the fountain standards are listed in Table I. The quantization magnetic field in the interrogation region is determined with a 0.1 nT uncertainty by measuring the frequency of a linear field-dependent "Zeeman" transition. The temperature in the interrogation region is monitored with 5 platinum resistors and the uncertainty on the black-body radiation frequency shift corresponds to temperature fluctuations of about 1 K [16]. Clock frequencies are corrected for the atom number-dependent frequency shifts using several methods [17, 18]. In DF_{Cs}, the cold collision shift is measured using a new method, based on state selection using an adiabatic passage, which we expose in the second part of this article. For DF_{Rb}, unlike [18], an optical molasses with a small number of atoms ($\sim 5.4 \times 10^6$) is used, while

TABLE I: Accuracy budget of the fountains involved in the 2002 measurements (DF et FOM).

Fountain	**DF_{Cs}**	**DF_{Rb}**	**FOM**
Effect	Value & Uncertainty (10^{-16})		
2^{nd} order Zeeman	1773.0 ± 5.2	3207.0 ± 4.7	385.0 ± 2.9
Blackbody Radiation	-173.0 ± 2.3	-127.0 ± 2.1	-186.0 ± 2.5
Cold collisions + cavity pulling	-95.0 ± 4.6	0.0 ± 1.0	-24.0 ± 4.8
Microwave spectrum	0.0 ± 2.0	0.0 ± 2.0	0.0 ± 1.7
Microwave leakage	0.0 ± 2.0	0.0 ± 2.0	0.0 ± 1.4
Residual first order Doppler	0.0 ± 2.0	0.0 ± 2.0	0.0 ± 2.0
Ramsey and Rabi pulling	< 1.0	< 1.0	< 1.0
Recoil	< 1.0	< 1.0	< 1.0
$2^n d$ Doppler effect	< 0.08	< 0.08	< 1.0
Background collisions	< 1.0	< 1.0	
Total uncertainty	**8**	**7**	**8**
Gravitational redshift	63.0 ± 1.0	63.0 ± 1.0	65.0 ± 1.0

keeping the microwave cavity tuned on resonance to better than 100 kHz. We thus estimate that the cavity pulling and the cold collsion shift are both smaller than 5×10^{-17}. All other effects do not contribute significantly. We searched for the influence of synchronous perturbations by changing the timing sequence and the atom launch height. To search for possible microwave leakage, we changed the power ($\times 9$) in the interrogation microwave cavity. No shift was found at a resolution of 10^{-15}. The shift due to residual coherences and populations in neighboring Zeeman states is estimated to be less than 10^{-16}. As shown in [19], the shift due to the microwave photon recoil is very similar for Cs and Rb and smaller than $+1.4 \times 10^{-16}$. Relativistic corrections (gravitational redshift and second order Doppler effect) contribute to less than 10^{-16} in the clock comparisons.

To compare the two Cs clocks running during the 2002 campaign, FOM and DF_{Cs}, we calculate the mean fractional frequency difference:

$$\frac{\nu_{Cs}^{DF}(2002) - \nu_{Cs}^{FOM}(2002)}{\nu_{Cs}} = +12(6)(12) \times 10^{-16} \quad (1)$$

where the first parenthesis reflects the 1σ statistical uncertainty, and the second the systematic uncertainty, obtained by adding quadratically the inaccuracies of the two Cs clocks (see Table I). We therefore find that the two Cs fountains are in good agreement despite their significantly different operating conditions (see Table I), showing that systematic effects are well understood at the 10^{-15} level. We then define the average cesium frequency ν_{Cs} as

$$\nu_{Cs} = \frac{\nu_{Cs}^{DF}(2002) + \nu_{Cs}^{FOM}(2002)}{2} \quad (2)$$

To measure the ^{87}Rb frequency, we first calculate the mean fractional frequency difference between FOM and DF_{Rb}. We obtain

$$\frac{\nu_{Rb}^{DF}(2002)}{\nu_{Rb}(1999)} - \frac{\nu_{Cs}^{FOM}(2002)}{\nu_{Cs}} = -7(4) \times 10^{-16} \quad (3)$$

where the parenthesis reflects the 1σ statistical uncertainty, which leads to

$$\frac{\nu_{Rb}^{DF}(2002)}{\nu_{Rb}(1999)} - 1 = -13(5) \times 10^{-16} \quad (4)$$

Finally, the ^{87}Rb frequency measured in 2002 with respect to the average ^{133}Cs frequency is found to be:

$$\nu_{Rb}(2002) = 6\,834\,682\,610.904\,324(4)(7)\,\text{Hz} \quad (5)$$

where the error bars now include DF_{Rb}, DF_{Cs} and FOM uncertainties. This is the most accurate frequency measurement to date.

In Fig.4 are plotted all our Rb-Cs frequency comparisons. Except for the less precise 1998 data [15], two Cs fountains were used together to perform the Rb measurements. The uncertainties for the 1999 and 2000 measurements were 2.7×10^{-15}, because of lower clock accuracy and lack of rigorous simultaneity in the earlier frequency comparisons [20]. A weighted linear fit to the data in Fig.4 determines how our measurements constrain a possible time variation of ν_{Rb}/ν_{Cs}. We find:

$$\frac{d}{dt} \ln\left(\frac{\nu_{Rb}}{\nu_{Cs}}\right) = (0.2 \pm 7.0) \times 10^{-16}\,\text{yr}^{-1} \quad (6)$$

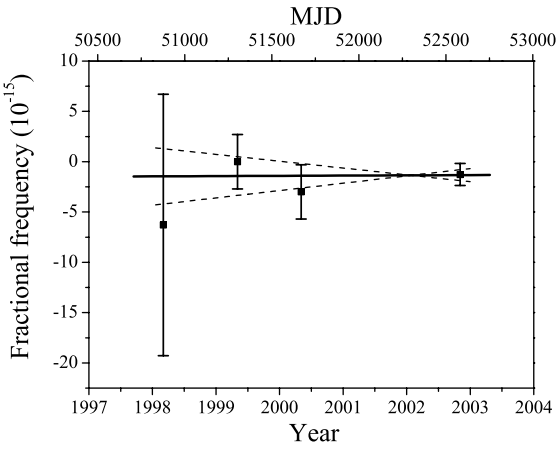

FIG. 4: Measured ^{87}Rb frequencies referenced to the ^{133}Cs fountains over 57 months. The 1999 measurement value ($\nu_{\rm Rb}(1999) = 6\,834\,682\,610.904\,333$ Hz) is conventionally used as reference. A weighted linear fit to the data gives $\frac{d}{dt}\ln\left(\frac{\nu_{\rm Rb}}{\nu_{\rm Cs}}\right) = (0.2 \pm 7.0) \times 10^{-16}\,{\rm yr}^{-1}$. Dotted lines correspond to the 1σ slope uncertainty.

which represents a 5-fold improvement over our previous results [20] and a 100-fold improvement over the Hg^+-H hyperfine energy comparison [11].

We now examine how this result constrains possible variations of fundamental constants. For an alkali with atom number Z, the hyperfine transition frequency can be approximated by:

$$\nu \propto \alpha^2 \frac{\mu}{\mu_N}\left(\frac{m_e}{m_p}\right) R_\infty c\, F_{rel}(Z\alpha), \qquad (7)$$

where R_∞ is the Rydberg constant, c the speed of light, μ the magnetic moment of the nucleus, μ_N the nuclear magneton. $F_{rel}(Z\alpha)$ is a relativistic function which strongly increases with Z [11, 21]. For ^{133}Cs, this Casimir relativistic contribution amounts to 40 % of the hyperfine splitting. Following [11] and neglecting possible changes of the strong and weak interactions affecting $\mu_{\rm Rb}$ and $\mu_{\rm Cs}$, a variation $\delta\alpha$ of the fine structure constant would change the ratio of two hyperfine frequencies according to the following equation

$$\delta\ln\left(\frac{\nu_2}{\nu_1}\right) = \left(\frac{\alpha}{F_2}\frac{\partial F_2}{\partial\alpha} - \frac{\alpha}{F_1}\frac{\partial F_1}{\partial\alpha}\right) \times \frac{\delta\alpha}{\alpha} \qquad (8)$$

where F_i stands for $F_{rel}(Z_i\alpha)$. The sensitivity of a frequency comparison to a change in α clearly depends on the value of the coefficients $\alpha\frac{\partial ln(F_{rel}(Z\alpha))}{\partial\alpha}$, which happen to also strongly increase with Z. A frequency comparison is more sensitive when the difference in the Z numbers of the two atoms is large. For ^{133}Cs, $\alpha\frac{\partial ln(F_{rel}(Z\alpha))}{\partial\alpha} = 0.74$. For ^{87}Rb, this quantity is 0.30 [22]. Finally, the sensitivity of the ratio $\nu_{\rm Rb}/\nu_{\rm Cs}$ to a variation of α is simply given by:

$$\frac{\partial}{\partial\ln\alpha}\ln\left(\frac{\nu_{\rm Rb}}{\nu_{\rm Cs}}\right) \simeq (0.30 - 0.74) = -0.44. \qquad (9)$$

Using equations 6 and 9, we thus set the new limit:

$$\dot{\alpha}/\alpha = (-0.4 \pm 16) \times 10^{-16}\,{\rm yr}^{-1}. \qquad (10)$$

In contrast with [11], Ref.[21] argues that a time variation of the nuclear magnetic moments must also be considered in a comparison between hyperfine frequencies. The magnetic moments μ can be calculated using the Schmidt model. For atoms with odd A and Z such as ^{87}Rb and ^{133}Cs, the Schmidt magnetic moment $\mu^{(s)}$ is found to depend only on g_p, the proton gyromagnetic ratio. With this simple model, Ref.[21] finds:

$$\frac{\partial}{\partial\ln g_p}\ln\left(\frac{\nu_{\rm Rb}}{\nu_{\rm Cs}}\right) \simeq \frac{\partial}{\partial\ln g_p}\ln\left(\frac{\mu^{(s)}_{\rm Rb}}{\mu^{(s)}_{\rm Cs}}\right) \simeq 2.0. \qquad (11)$$

Attributing any variation of $\nu_{\rm Rb}/\nu_{\rm Cs}$ to a variation of g_p, equations 6 and 11 lead to: $\dot{g_p}/g_p = (0.1 \pm 3.5) \times 10^{-16}\,{\rm yr}^{-1}$. However, it must be noted that the Schmidt model is over simplified and does not agree very accurately with the actual magnetic moment.

Moreover, attributing all the time variation of $\nu_{\rm Rb}/\nu_{\rm Cs}$ to either g_p or α independently is somewhat artificial. Theoretical models allowing for a variation of α also allow for variations in the strength of the strong and electroweak interactions. For instance, Ref.[5] argues that Grand unification of the three interactions implies that a time variation of α necessarily comes with a time variation of the coupling constants of the other interactions. Ref.[5] predicts that a fractional variation of α is accompanied with a ~ 40 times larger fractional change of m_e/m_p. In order to independently test the stability of the three fundamental interactions, several comparisons between different atomic species and/or transitions are required. For instance and as illustrated in [23], absolute frequency measurements of an optical transition versus a hyperfine one is sensitive to a different combination of fundamental constants: $(\mu_{\rm Cs}/\mu_N)(m_e/m_p)\alpha^x$, where x depends on the particular atom and/or transition.

A more complete theoretical analysis going beyond the Schmidt model would clearly be very useful to interpret frequency comparisons involving hyperfine transitions. This is especially important as most precise frequency measurements, both in the microwave and the optical domain [23–25], are currently referenced to the ^{133}Cs hyperfine splitting, the basis of the SI definition of the second. The H hyperfine splitting, which is calculable to a high accuracy, has already been considered as a possible reference several decades ago. Unfortunately, despite numerous efforts, the H hyperfine splitting is currently measured to only 7 parts in 10^{13} (using H-masers), almost three orders of magnitude worse than the results presented in this article.

Finally, an unambiguous test of the stability of α should be possible by comparing two optical transitions. Indeed, the frequency of an electronic transition depends only on the fine structure constant : it can be expressed as $\nu_{opt} = Ry \times f(\alpha)$, where $f(\alpha)$ includes relativistic effects, many-body effects, spin-orbit coupling. We anticipate major advances in these tests using frequency standards, thanks to recent advances in optical frequency metrology using femtosecond lasers [23, 26].

To improve significantly and quickly the quality of our test, fountain clocks of better accuracy are required. As shown in Table I, the relative accuracy of the Cs fountain clocks, presently slightly better than $\sim 10^{-15}$, is mostly limited by the uncertainty on the quadratic Zeeman shift and the cold collision frequency shift [27, 28]. The Zeeman shift can easily be evaluated with a better accuracy by monitoring more frequently the magnetic field. The cold collision shift is commonly measured with a 10 to 20 % systematic and statistical uncertainty only [29, 30]. To reach an accuracy better than 10^{-15}, one could in principle operate with a small number of detected atoms, say 10^5, for which the cold collision shift is about 10^{-15} only. But this sets a standard quantum limit to the frequency stability [31] of about $10^{-13}\tau^{-1/2}$, where τ is the averaging time in seconds. With such a stability, the evaluation of all the systematic effects at the 10^{-16} level is not practicable. However, when using a high number of atoms ($10^6 - 10^7$), a stability approaching $3 \times 10^{-14}\tau^{-1/2}$ has already been demonstrated [30, 31], which would make the evaluation at the 10^{-16} level practicable. Under these conditions, the cold collision frequency shift is very large ($10^{-14} - 10^{-13}$). In most experiments, a precise control of the atomic density is hard to achieve, which sets a limit to how accurately systematic effects due to collisions can be corrected for. This is particularly true for clocks using laser cooled Cs atoms [32, 33].

In this article, we present a method using adiabatic passage (AP) [34, 35] that allows to prepare atomic samples with well defined density ratios. This enables the determination of the collisional frequency shift at the percent level or better, in an atomic clock or atom interferometer.

In a fountain, the collisional frequency shift can be expressed as $\delta\nu_{col} = K_{coll} n_{eff}$, where K_{coll} is a constant that depends on the collisional parameters, and n_{eff} the effective density, as defined in [18]. n_{eff} is the time-averaged atomic density, weighted by the sensitivity function, which is averaged over the trajectories of the atoms that are effectively detected. It thus depends on many parameters : the initial number of atoms N, the rms size of the sample σ, its temperature T, the microwave power in the Ramsey cavities, the fountain geometry (through the size and position of the diaphragms), and the geometry of the detection zone. Unfortunately, n_{eff} can't be directly measured. It can be computed numerically though, by performing a Monte Carlo simulation of the expansion of the cloud in the fountain. The result of such a simulation happens to be very sensitive to the modelling of the velocity distribution, and to the actual values of the parameters of the fountain, which cannot be measured with a great accuracy. Still, this density is proportional to the number of detected atoms N_{det}. As a consequence, the collisional frequency shift can be written as $\delta\nu_{col} = K N_{det}$, where the coefficient K depends on all the parameters mentioned above.

The measurement of the cold collision shift is based on a differential method [18]. One alternates sequences of measurements with two different, high and low atomic densities, (HD and LD). The frequency difference between the two situations, as well as the difference in the number of detected atoms, are measured. Alternating the measurements each 100 cycles allow to efficiently reject fluctuations and drifts of the maser frequency, so that the difference in the clock frequencies corresponds to the difference in the collisional shifts between the two configurations, which can be written as

$$\delta\nu_{coll}^{HD} - \delta\nu_{coll}^{BD} = K^{HD} N_{det}^{HD} - K^{LD} N_{det}^{LD} \qquad (12)$$

In the case where the coefficients K^{HD} and K^{LD} are

identical the differential shift can be factorized

$$\delta\nu_{coll}^{HD} - \delta\nu_{coll}^{BD} = K(N_{det}^{HD} - N_{det}^{LD}) \qquad (13)$$

This allows to measure the K coefficient. A linear extrapolation of the clock frequency to zero detected atoms then gives the corrected frequency ν_0

$$\nu_0 = \nu^{HD} - KN_{det}^{HD} \qquad (14)$$

It is also important to notice that an absolute determination of K is not necessary. A relative determination of the number of detected atoms is enough to extrapolate the corrected frequency.

Up to now, two methods have been used to change the density, and hence the number of detected atoms N_{det}. Atoms are initially loaded in an optical molasses, whose parameters (duration, laser intensity) can be varied. An other technique consists in keeping the same loading parameters but changing the power in a selection microwave cavity, which is used to prepare atoms in the $|F = 3, m_F = 0\rangle$ state. One can select all (resp. half) of the atoms initially in the $|F = 4, m_F = 0\rangle$ state by applying a π (resp. $\pi/2$) pulse and pushing away the atoms remaining in the $|F = 4\rangle$ state. However, due to the microwave field inhomogeneities in the cavity, the pulses cannot be perfectly π and $\pi/2$ pulses for all the atoms. Besides affecting the atomic densities, both techniques also affect position and velocity distributions, as well as collisional energy, and consequently the K coefficients usually differ for the low and high density cases. Our numerical simulation, which takes into account the fountain geometry, the position and velocity distributions of the atomic cloud, shows that, for these methods, a linear extrapolation leads in the best case to a 10-20 % error in the determination of the collisional shift. Fluctuations and imperfect determination of those parameters prevent from performing an accurate evaluation of the K coefficient. Moreover, for cesium atoms, as the collisional shift is energy dependent [36], this error can even be larger.

A method immune against these systematic effects prescribes to change the number of atoms of the sample without changing neither its velocity distribution, nor its size. This can be realized by an adiabatic transfer of population, which allows one to prepare two atomic samples, where both the ratio of the effective densities and the ratio of the atom numbers are exactly 1/2. In contrast to previous methods, this one is insensitive to fluctuations of experimental parameters such as the size and temperature of the atomic sample, or the power coupled into the selection cavity.

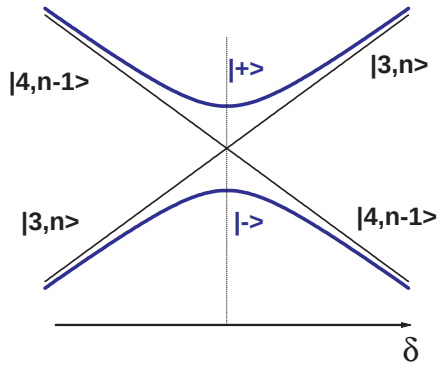

FIG. 5: Energies of the dressed levels as a function of the detuning from resonance.

For a two-level atom interacting with a microwave field, the interaction hamiltonian is

$$\mathbf{H_R} = \frac{\hbar}{2}\begin{pmatrix} \delta & \Omega \\ \Omega & -\delta \end{pmatrix}$$

where δ is the detuning with respect to resonance, and $\Omega/2\pi$ the Rabi frequency. It describes the evolution of the quantum state $|\Psi\rangle$ in the basis of the initial hyperfine states $|F = 3\rangle$ and $|F = 4\rangle$. In a dressed state picture, the eigenstates of the two state hamiltonian read

$$|+\rangle = \sin\theta|3, n\rangle + \cos\theta|4, n-1\rangle \qquad (15)$$

$$|-\rangle = \cos\theta|3, n\rangle - \sin\theta|4, n-1\rangle \qquad (16)$$

where

$$\mathrm{cotg}(2\theta) = -\frac{\delta}{\Omega} \qquad (17)$$

Both the mixing angle θ and the eigenenergies are a function of the detuning δ, as shown on figure 5. If δ is swept across resonance, the mixing angle θ turns from 0 to $\pi/2$, and consequently $|+\rangle$ evolves from $|4, n-1\rangle$ to $|3, n\rangle$.

To insure that the state $|\Psi\rangle$ follows the dressed state $|+\rangle$ adiabatically during the interaction, the following adiabaticity condition has to be fulfilled

$$\left| < -|\frac{\partial|+\rangle}{\partial t}\right| \ll \frac{\Delta E}{\hbar} \qquad (18)$$

where ΔE is the difference between the eigenenergies.

It can also be written as

$$\left|\Omega\frac{\partial\delta}{\partial t} - \delta\frac{\partial\Omega}{\partial t}\right| \ll 2(\Omega^2+\delta^2)^{3/2} \tag{19}$$

This condition is the most stringent in the vicinity of the crossing, where it reduces to

$$\left|\dot{\delta}(t)\right| \ll \Omega^2(t). \tag{20}$$

In order to fulfill the adiabaticity condition, we choose to chirp the detuning from resonance δ according to

$$\dot{\delta}(t) \propto \Omega^2(t). \tag{21}$$

First, an adiabatic passage in the selection cavity is used to transfer with a 100% efficiency all the atoms from the $|F=4, m_F=0\rangle$ state to the $|F=3, m_F=0\rangle$ state [34, 35]. This requires that the frequency of the microwave field in the cavity is swept across resonance, and that the Rabi frequency $\Omega(t)/2\pi$ has an appropriate shape and maximum value, $\Omega_{max}/2\pi$. We use Blackman pulses (BP), which minimize off-resonance excitation [37]. Figure 6 shows the evolution of the microwave field amplitude together with the frequency chirp.

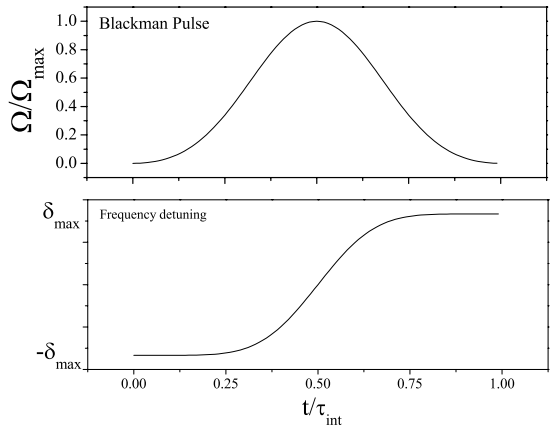

FIG. 6: Temporal dependence of the Blackman pulse and the corresponding frequency chirp.

Second, we exploit another striking property of AP : if we stop the AP sequence when $\delta = 0$ (half-Blackman pulse HBP), the atoms are left in a superposition of the $|F=4, m_F=0\rangle$ and $|F=3, m_F=0\rangle$ states, with weights rigourously equal and independent of the Rabi frequency. After removal of the $|F=4\rangle$ atoms with a pushing laser beam, half of the atoms are in the $|F=3, m_F=0\rangle$ state, as desired.

One can in principle obtain any transition probability between 0 and 1 by stopping the frequency chirp at the proper detuning. But in general, the transition probability depends on the final Rabi frequency. It would then be different for atoms located at different positions in the selection microwave cavity. Only BP and HBP provide a transition probability independent of the Rabi frequency.

In order to optimize this AP method and to evaluate its sensitivity to experimental parameters, we first performed a simple numerical simulation, solving the time-dependent Schrödinger equation for a two level atom in a homogeneous microwave field. The choice of the pulse parameters comes from a compromise between the insensitivity of the transition probabilities to fluctuations of the microwave power and the parasitic excitation of non-resonant Zeeman transitions. Figure 7 displays the calculated transition probabilities as a function of the maximum Rabi frequency $\Omega_{max}/2\pi$, for BP and HBP. The parameters were a duration $\tau_{int} = 4$ ms, and $\delta_{max}/2\pi = 5$ kHz, which were constant over the course of the experiment. The simulation shows that the transition probabilities deviate from 1 and 1/2 by less than 10^{-3} as soon as $\Omega_{max}/2\pi$ is larger than 2.4 kHz.

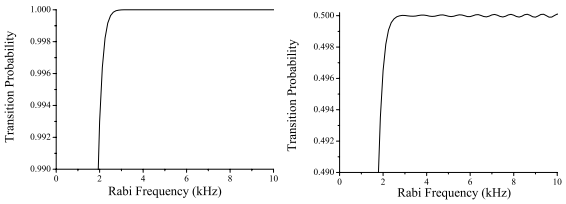

FIG. 7: Transition probabilities for a BP and a HBP as a function of the maximal Rabi frequency $\Omega_{max}/2\pi$. The parameters are $\tau_{int} = 4$ ms and $\delta_{max}/2\pi = 5$ kHz.

We finally performed a complete simulation, which takes into account the gaussian spatial distribution of the atomic cloud (characterized by its rms size $\sigma = 3.5$ mm) and its trajectory, as well as the microwave field (longitudinal and transverse) distribution of the TE_{011} mode for our cylindrical selection cavity.

To investigate the influence of the actual position and trajectory of the cloud inside the microwave cavity

during the pulse (the cloud travels over about 16 mm during a 4 ms long pulse), we calculate the transition probability for an atom travelling along the symmetry axis of the cavity and undergoing a BP or a HBP as a function of its location in the cavity at the beginning of the pulse. The result of this calculation for a BP is shown on figure 8. The simulation indicates that

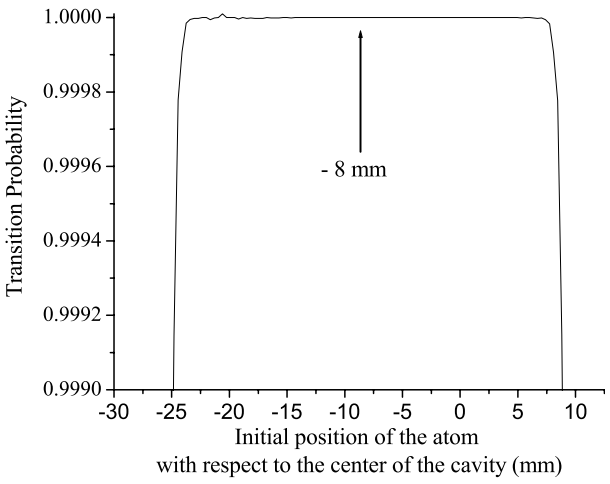

FIG. 8: Transition probabilities for a BP as a function of the initial position of the atom with respect to the center of the microwave cavity. The maximal Rabi frequency (at the center of the cavity) is $\Omega_{max}/2\pi = 7.5$ kHz. The parameters are $\tau_{int} = 4$ ms and $\delta_{max}/2\pi = 5$ kHz.

the transition probability deviates from 1 by less than 10^{-3} for atoms distributed over about 33 mm. This corresponds to atoms within about $\pm 5\sigma$ of the vertical spatial distribution, provided the center of the cloud is located 8 mm below the center of the cavity at the beginning of the pulse (this position is indicated by the arrow on figure 8). Under this condition, the atomic cloud is located at the center of the cavity at the middle of the BP, where the Rabi frequency is maximal.

The result of this calculation for a HBP is shown on figure 9. The simulation indicates that the transition probability deviates from the ideal value by less than 10^{-3} for all the atoms contained within $\pm 3.5\sigma$ of the vertical spatial distribution (more than 99.95 % of the atoms in the cloud). The simulation indicates that in order to minimize the sensitivity of the transfer efficiency to microwave field inhomogeneities and timing errors, the center of the cloud has to be located in the center of the cavity at the end of the HBP. For our parameters, this means that the center of the cloud at

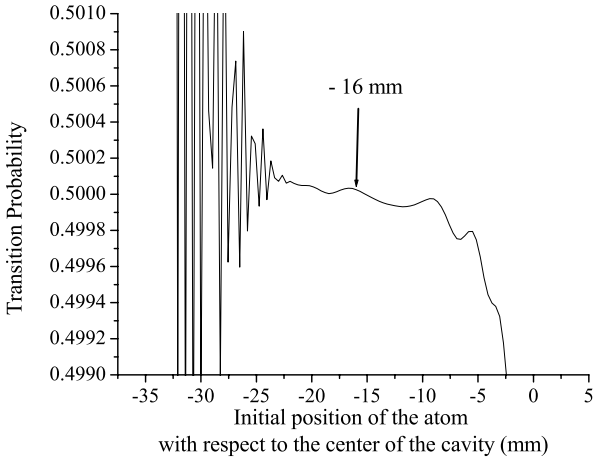

FIG. 9: Transition probabilities for a HBP as a function of the initial position of the atom with respect to the center of the microwave cavity. The maximal Rabi frequency (at the center of the cavity) is $\Omega_{max}/2\pi = 7.5$ kHz. The parameters are $\tau_{int} = 4$ ms and $\delta_{max}/2\pi = 5$ kHz.

the beginning of the pulse has to be located 16 mm below the center of the cavity (see the arrow on figure 9). For instance, a delay as large as 1 ms with respect to the optimal timing induces only a 7×10^{-5} variation on the transition probability.

The only critical parameter is the accuracy of the detuning at the end of the chirp for HBP. We calculated the sensitivity of the transition probability to the final detuning. The results for two different maximum Rabi frequencies are shown in figure 10. We find a linear sensitivity of the transition probability to the final detuning of 6.9×10^{-5}/Hz for $\Omega_{max}/2\pi = 7.5$ kHz.

We use our double fountain (DF_{Cs}) to demonstrate the AP method and the resulting ability to control the collisional shift. This clock is an improved version of the Rb fountain already described elsewhere [15, 30]. The principle of operation of this clock has already been explained above. We therefore give here only some relevant details. In contrast with the Rb fountain where the optical molasses was loaded from a vapor, we use here a laser slowed atomic beam to increase the loading rate. About 10^9 atoms are gathered within 800 ms in a lin $\perp$ lin optical molasses, with 6 laser beams tuned to the red of the $F = 4 \rightarrow F' = 5$ transition at 852 nm. The atoms are then launched upwards at ~ 4.1 m/s within 2 ms, and cooled down to an effective temperature of $\sim 1\mu$K. After launch,

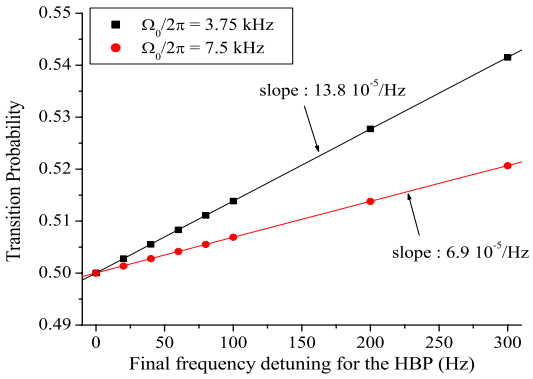

FIG. 10: Transition probabilities for a HBP (with $\tau_{int} = 4$ ms, $\delta_{max}/2\pi = 5$ kHz) as a function of the final frequency. The results are displayed as squares and circles. The lines are the results of the fits to the data.

the atoms are prepared into the $|F = 3, m_F = 0\rangle$ state using a combination of microwave and laser pulses : they first enter the selection cavity ($Q \sim$1000) tuned to the $|F = 4, m_F = 0\rangle \rightarrow |F = 3, m_F = 0\rangle$ transition, where they experience either BP or HBP pulses. The atoms left in the $F = 4$ state are pushed away by a laser beam tuned to the $F = 4 \rightarrow F' = 5$ transition, 10 cm above the selection cavity. The amplitude of the Blackman pulses are shaped by applying an adequate voltage sequence (500 steps) to a microwave voltage-controlled attenuator (60 dB dynamic range), whereas the frequency chirp is performed with a voltage controlled oscillator. The Rabi frequency profile agrees with the expected Blackman shape within a few percent. The frequency chirp, and more specifically its final frequency, was not verified as it cannot be easily checked at the required precision level of 10 Hz for HBP. After the selection, the atoms interact with a resonant microwave field according to the Ramsey interrogation scheme, and are finally detected by fluorescence, as already explained before.

The transition probabilities in the selection cavity are first measured as a function of the maximum Rabi frequency $\Omega_{max}/2\pi$, for the Blackman and half-Blackman pulses. In this evaluation phase only, the pushing beam has to be off. To reject the fluctuations of the initial number of atoms, we measure the ratio of the atoms transferred into $|F = 3, m_F = 0\rangle$ and the total number of detected atoms, in all magnetic sublevels. The transfer probability is then obtained by dividing the measured ratio by the initial fraction of atoms in the $|F = 4, m_F = 0\rangle$ state. The results are shown in figure 11 and reproduce very well the numerical simulations.

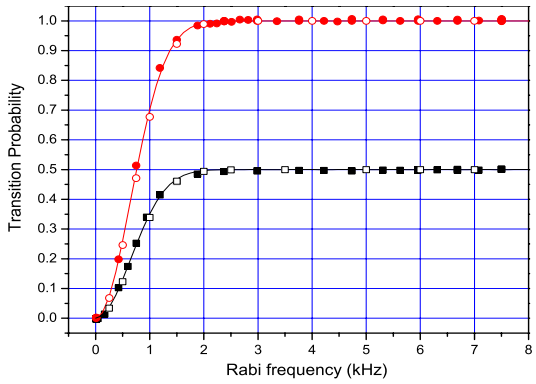

FIG. 11: Transition probabilities for a BP and a HBP with $\tau_{int} = 4$ ms, $\delta_{max}/2\pi = 5$ kHz as a function of $\Omega_{max}/2\pi$. The results of the numerical simulations are displayed as lines (homogeneous Rabi frequency case) and open symbols (TE011 cavity case), whereas the measurements are full symbols.

As the maximum Rabi frequency during the experiment was set to 7.5 kHz, the resonance frequencies for transitions between $m_F \neq 0$ states have to be significantly shifted away from the 0-0 transition. A magnetic field of $\sim$ 180 mG is applied during the pulses which keeps the total parasitic excitation of magnetic field sensitive transitions below 0.3 %. This pulse induces a transient quadratic Zeeman shift on the 0-0 transition of about 14 Hz than must be taken into account to meet the resonance condition for HBP.

We alternatively measure the mean atom number for the Blackman and half-Blackman pulses during sequences of 50 fountain cycles, and compute their ratio R. We then calculate R_N, the average of R for N successive sequences. In figure 12, the standard deviation $\sigma_R(N)$ for various N is plotted. The stability of R reaches 3×10^{-4} after a one-day integration. This reflects the insensitivity of the AP to the experimental parameter fluctuations. The mean value of the ratio is $R = 0.506$, whereas it was expected to be 0.5 at the 10^{-3} level. This deviation cannot be explained by a non-linearity of the detection, which could arise from absorption in the detection beams. When the absorption in the detection laser beams is changed by a factor 2, by changing the power of the beams, we observe no change in the ratio larger than 10^{-3}. We attribute this deviation to the uncertainty in the final frequency of

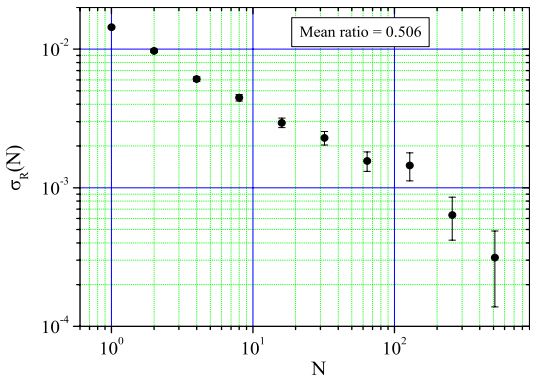

FIG. 12: Standard deviation of the fluctuation of the ratio R, as a function of the number N of successive sequences of measurements.

the sweep. In our present set-up, the sweep is generated by an oscillator whose specified accuracy is limited to 50 Hz for a frequency sweep from -5 to +5 kHz (this difficulty can be solved by using a dedicated DDS numerical synthesizer). We measured the transition probability as a function of the offset frequency at the end of the HBP (see figure 13), and find a linear deviation in the transition probability of $7.6(2) \times 10^{-5}$/Hz in reasonable agreement with the predicted value. A

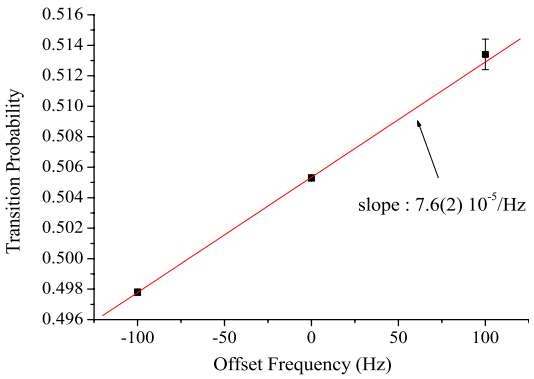

FIG. 13: Transition probabilities for a HBP (with $\tau_{int} = 4$ ms, $\delta_{max} = 5$ kHz) measured as a function of the final frequency. The results are displayed as squares. The line is the result of a fit to the data.

50 Hz deviation can explain a deviation of the ratio by about 4×10^{-3}. However, it is important to notice that even when the final frequency is detuned by 50 Hz, the spatial variation of the transition probability across the atomic sample is less than 10^{-3}. All the tests performed here demonstrate that AP is at least accurate at the 1% level.

Measurements of the collisional frequency shift are then carried out using BP and HBP pulses. In order to amplify the collisional shift, the number of detected atoms ($N_{det} \sim 10^7$) is about 10 times larger than needed in order to operate the clock in optimal conditions. From a differential measurement, one can extrapolate the frequency ν_0 of the clock at zero density with respect to the H-maser. The relative resolution of the frequency difference is $2 \times 10^{-13}\tau^{-1/2}$, limited by the phase noise of the quartz oscillator used for the fountain interrogation. To check whether this extrapolation is correct, we measure the corrected frequency ν_0 for two different initial temperatures of the atomic cloud, 1.1 and 2.3 μK, for which the effective densities, number of detected atoms and K coefficients are expected to be different. We switch every 50 cycles between four different configurations : 1.1 μK and BP, 1.1 μK and HBP, 2.3 μK and BP, 2.3 μK and HBP. This rejects long term fluctuations in the experiment induced by frequency drift of the H-maser used as a reference, variation of the detection responsivity, and fluctuations of other systematic effects.

The results are summarized in table II. For each configuration, the measurement of the clock frequency and number of atoms is averaged over a total time of about 50 hours. One can then extract the difference between the high and low density collisional shifts $\delta\nu_{diff}$ with a relative resolution of 5×10^{-16}. The K constants are found to differ by about 20 %. The corrected frequency ν_0 is then simply obtained by subtracting $\delta\nu_{diff}$ to the measured clock frequency in the low density configuration. The difference between the corrected frequencies $\delta\nu_0$ can then be estimated. The uncertainty on this measurement is two-fold, a statistical uncertainty, and a systematic error which reflects the 1 % uncertainty on the ratio R. The difference between the corrected frequencies is found to be $\delta\nu_0 = -0.012(7)(5)$ mHz. This difference is less than 2 % of the collisional shift at high density. The difference is compatible with zero within the error bars, showing that the extrapolation to zero detected atoms is correct.

It is also important to notice that we measure simultaneously the collisional frequency shift and the shift due to cavity pulling [20], which is proportional to the number of atoms crossing the Ramsey cavity. Both effects are correctly evaluated by our method.

TABLE II: Measurement of the cold collisional frequency shift using Adiabatic Passage for two atomic temperatures T. The first (resp. second, when present) error bar indicated in parenthesis reflects the statistical (resp. systematic) uncertainty.

T	$\delta\nu_{diff}$ (mHz)	R	K ($\times 10^{-11}$) Hz/at
1.1μK	-0.323(5)	0.5063(3)	-8.62(13)
2.3μK	-0.260(5)	0.5056(3)	-10.04(20)

Difference in corrected frequency $\delta\nu_0$: -0.012(7)(5) mHz

To compare the standard selection method (SSM) and AP, we perform a measurement alternating both methods for selection. Table III displays the results obtained for a temperature of $1.1\mu K$. The K coefficients are found to differ by about 10%. Indeed, when using a $\pi/2$ pulse with the standard selection, the density distribution is transversally distorted : atoms along the symmetry axis of the cavity are more efficiently transferred than off-axis atoms. This increases the effective density for the same number of detected atoms with respect to AP, giving a larger collision shift at low density. In fact, K is expected to be lower with SSM than AP, in agreement with our measurement. Extrapolating the frequency to zero density when using SSM then leads to an error of about 7×10^{-15} at this density.

TABLE III: Comparison between the Adiabatic Passage technique (AP) and the Standard Selection Method (SSM). The temperature of the sample for these measurements was 1.1μK.

	$\delta\nu_{diff}$ (mHz)	R	K ($\times 10^{-11}$) Hz/at
SSM	-0.234(7)	0.540(3)	-8.08(24)
AP	-0.275(8)	0.5054(8)	-8.97(23)

More recently, we compared AP with the technique which consists in changing the loading duration to change the number of atoms. In the following, we refer to this last method as LDM : Loading Duration Method. The results are displayed in Table IV. The ratio for AP is measured to be 0.5009(4), closer from 0.5. We attribute this change to the use of a different RF synthetizer for the AP. The K coefficients are found to differ by about 15 %. Extrapolating the frequency to zero density when using LDM then leads to an error of about 1.5×10^{-14} at this density. Note that for this measurement, the value of the K coefficient for AP significantly differs from our previous measurement. This can be due to an imperfect calibration of the number of detected atoms.

TABLE IV: Comparison between the Adiabatic Passage technique (AP) and the Loading Duration Method (LDM). The temperature of the sample for these measurements was about 1μK.

	$\delta\nu_{diff}$ (mHz)	R	K ($\times 10^{-11}$) Hz/at
LDM	-0.556(4)	0.507(3)	-22.1(2)
AP	-0.489(4)	0.5009(4)	-19.1(2)

In the near future, accuracies near 1 part in 10^{16} should be achievable in microwave atomic fountains, which would improve our present Rb-Cs comparison by one order of magnitude. To reach such an accuracy, the cold collisional shift has to be carefully evaluated. We demonstrate here a new method based on an adiabatic transfer of population to prepare atomic samples with a well-controlled density ratio. This method can lead to a potential control of the cold collision shift at the 10^{-3} level. This capability could be demonstrated by using an ultra stable cryogenic oscillator [31], allowing a frequency resolution of 10^{-16} per day. Using this method, the evaluation of the Cs fountain accuracy at the 10^{-16} level is reachable.

By comparing ^{133}Cs and ^{87}Rb hyperfine energies, we have set a stringent upper limit to a possible fractional variation of the quantity $(\mu_{\rm Rb}/\mu_{\rm Cs})\alpha^{-0.44}$ at $(-0.2 \pm 7.0) \times 10^{-16}{\rm yr}^{-1}$. A further step is the extension of these comparisons for distant clocks in different laboratories in the world. Serving this purpose, a new generation of time/frequency transfer at the 10^{-16} level is currently under development for the ESA space mission ACES which will fly ultra-stable clocks on board the international space station in 2006 [38]. These comparisons will also allow for a search of a possible change of fundamental constants induced by the annual modulation of the Sun gravitational potential due to the elliptical orbit of the Earth [39].

Acknowledgments: The authors wish to thank A. Gérard, and the electronic staff for technical assistance, and P. Wolf, J.P. Uzan, T. Damour for fruitful discussions. This work was supported in part by BNM and CNRS. BNM-SYRTE and Laboratoire Kastler-Brossel are Unités Associées au CNRS, UMR 8630 and 8552.

* Present address: Istituto Elettrotecnico Nazionale G. Ferraris , Strada delle Cacce 41, 10135 Torino, Italy
† Present address: Institutul National de Fizica Laserilor, Plasmei si Radiatiei, P.O. Box MG36, Bucaresti, Magurele, Romania

[1] P.A.M. Dirac, Nature **139**, 323 (1937).
[2] F. Dyson, in *Current trends in the theory of fields*, (AIP New-York, 1983), p. 163.
[3] For a review, see for instance J.P. Uzan, Rev. Mod. Phys. **75**, 403 (2003), and references therein.
[4] T. Damour and A. Polyakov, Nucl. Phys. B **423**, 532 (1994); T. Damour, F. Piazza, and G. Veneziano, Phys. Rev. Lett. **89**, 081601 (2002).
[5] X. Calmet and H. Fritzsch, Eur. Phys. J. C **24**, 639 (2002).
[6] T. Damour and F. Dyson, Nucl. Phys. B **480**, 37 (1996).
[7] A.V. Ivanchik, E. Rodriguez, P. Petitjean and D.A. Varshalovich, Astron. Lett. **28**, 423 (2002).
[8] J.K. Webb *et al.*, Phys. Rev. Lett. **87**, 091301 (2001).
[9] J.P. Turneaure *et al.*, Phys. Rev. D **27**, 1705 (1983).
[10] A. Godone, C. Novero, P. Tavella and K. Rahimullah, Phys. Rev. Lett. **71**, 2364 (1993).
[11] J.D. Prestage, R.L. Tjoelker and L. Maleki, Phys. Rev. Lett. **74**, 3511 (1995).
[12] V.A. Dzuba, V.V. Flambaum and J.K. Webb, Phys. Rev. A **59**, 230 (1999).
[13] A. Clairon *et al.*, in *Proc. of the 5^{th} Symposium on Frequency Standards and Metrology*, ed. J. Bergquist (World Scientific, Singapore, 1995), p. 49.
[14] S. Bize *et al.*, in *Proc. of the 6^{th} Symposium on Frequency Standards and Metrology* (World Scientific, Singapore, 2001), p 53.
[15] S. Bize *et al.*, Europhys. Lett. **45**, 558 (1999).
[16] E. Simon *et al.*, Phys. Rev. A **57**, 436 (1998).
[17] F. Pereira Dos Santos *et al.*, Phys. Rev. Lett. **89**, 233004 (2002).
[18] Y. Sortais *et al.*, Phys. Rev. Lett. **85**, 3117 (2000).
[19] P. Wolf *et al.*, in *Proc. of the 6^{th} Symposium on Frequency Standards and Metrology* (World Scientific, Singapore, 2001), p 593.
[20] S. Bize, Y. Sortais, C. Mandache, A. Clairon, and C. Salomon, IEEE Trans. on Instr. and Meas. **50**, 503 (2001)
[21] S.G. Karshenboïm, Can. J. Phys. **47**, 639 (2000).
[22] A more precise calculation in [12] gives $LdF_{rel}(^{133}\mathrm{Cs}) = 0.83$, which differs by 10% from the Casimir formula.
[23] S. Bize *et al.*, Phys. Rev. Lett. **90**, 150802 (2003) , (2002).
[24] M. Niering *et al.*, Phys. Rev. Lett. **84**, 5496 (2000).
[25] Th. Udem *et al.*, Phys. Rev. Lett. **86**, 4996 (2001).
[26] See for instance *Proc. of the 6^{th} Symposium on Frequency Standards and Metrology* (World Scientific, Singapore, 2001).
[27] K. Gibble and S. Chu, Phys. Rev. Lett. **70**, 1771 (1993)
[28] S. Ghezali, P. Laurent, S. N. Lea, and A. Clairon, Europhys. Lett. **36**, 25 (1996)
[29] Y. Sortais *et al.*, Physica Scripta **95**, 50 (2001)
[30] S. Bize *et al.*, in Proceedings of 6th Symposium on Frequency Standards and Metrology (World Scientific), 53 (2001)
[31] G. Santarelli *et al.*, Phys. Rev. Lett. **82**, 4619 (1999)
[32] C. Chin, V. Leiber, V. Vuletić, A. J. Kerman, and S. Chu, Phys. Rev. A **63**, 033401 (2001)
[33] M. Bijlsma, B. J. Verhaar, and D. J. Heinzen, Phys. Rev. A **49**, R4285 (1994)
[34] A. Messiah, Quantum Mechanics, **2**, 637 (1959)
[35] M. M. T. Loy, Phys. Rev. Lett. **32**, 814 (1974)
[36] P. J. Leo, P. S. Julienne, F. H. Mies, and C. J. Williams, Phys. Rev. Lett. **86**, 3743 (2001)
[37] M. Kasevich, S. Chu, Phys. Rev. Lett. **69**, 1741 (1992)
[38] C. Salomon *et al.*, C. R. Acad. Sci. Paris, t.2, Série IV, 1313 (2001).
[39] A. Bauch and S. Weyers, Phys. Rev. D **65**, 081101 (R) (2002).